

Calculations for nuclear matter and finite nuclei within and beyond energy–density–functional theories through interactions guided by effective field theory

C.-J. Yang,^{1,2} W.G. Jiang,¹ S. Burrello,³ and M. Grasso⁴

¹*Department of Physics, Chalmers University of Technology, SE-412 96, Göteborg, Sweden*

²*Nuclear Physics Institute of the Czech Academy of Sciences, 25069 Řež, Czech Republic*

³*Institut für Kernphysik, Technische Universität Darmstadt, 64289 Darmstadt, Germany*

⁴*Université Paris-Saclay, CNRS/IN2P3, IJCLab, 91405 Orsay, France*

We propose a novel idea to construct an effective interaction under energy-density-functional (EDF) theories which is adaptive to the enlargement of the model space. Guided by effective field theory principles, iterations of interactions as well as enlargements of the model space through particle-hole excitations are carried out for infinite nuclear matter and selected closed-shell nuclei (^4He , ^{16}O , ^{40}Ca , ^{56}Ni and ^{100}Sn) up to next-to-leading order. Our approach provides a new way for handling the nuclear matter and finite nuclei within the same scheme, with advantages from both EDF and *ab initio* approaches.

INTRODUCTION

One important challenge in the nuclear many-body problem concerns the construction of interactions. Existing state-of-the-art approaches can be mainly categorized into two extremes: one starts with bare nucleon-nucleon (NN) degrees of freedom and improves the results order by order following effective-field-theory (EFT) [1–14] through *ab initio* calculations [15–24]; the other adopts the energy-density-functional (EDF) framework to build an “in medium” interaction within the self-consistent mean-field (MF) approximation. However, both approaches suffer from longstanding shortcomings.

Indeed, although *ab initio* approaches allow to construct the interaction on a clear foundation, they still suffer from technical difficulties concerning the reduction of the enormous model space required to converge the many-body calculations [25–37]. Attempts along this direction have been carried out through methods of unitary transformations [35–37] or an EFT procedure which accounts for both ultraviolet and infrared truncations [25–33]. Moreover, much effort has been spent to face theoretical problems related to the power counting issues [38–41] and the growing importance of three- and four-nucleon forces with the number of particles in the system [42–44]. Nonetheless, a definite solution to these questions is far from being assured.

On the other hand, a strong model-dependence characterizes the effective interactions usually employed in the EDF framework, as derived at the MF level. To complicate matters, it is known that beyond MF (BMF) effects need also to be taken into account. In contrast to the non-perturbative treatment adopted in *ab initio* calculations, approaches such as the MF Hartree-Fock approximation or BMF methods are then applied (see for instance Refs. [45–54]). However, BMF effects are usually evaluated by employing the same interaction fitted at MF, which generates an overcounting of correlations at

the BMF level. More refined methods exist to overcome this problem, such as self-energy-subtraction procedures, which are used for example in the second random-phase approximation [45]. Nevertheless, there is a lack of an order-by-order organization scheme to generate effective interactions applicable to both nuclear matter and finite nuclei. Even more importantly, as a common drawback of both EDF and *ab initio* approaches, the interaction is defined in a fixed model space—which stays *unchanged* throughout all considered orders.

Inspired by recent efforts toward bridging EDF and EFT ideas [55–88], we probe in this work a novel possibility—which proposes to improve *both* the interaction and the model space order by order. Specifically, we assume there is an underlying EFT expansion where the MF results correspond to the LO contribution. Subleading corrections are then added, which contain the iterated LO interaction renormalized in an enlarged model space through particle-hole excitations. Constructing an EFT in this direction naturally leads to a novel setup which demands:

- The interaction to be adaptive to the growth of the model space at each order.
- Iterations of LO interactions to be performed through an in-medium propagator.

This strategy was already applied to infinite matter for instance in Refs. [58, 62, 65, 75]. Note that an attempt to include the second-order Dyson diagrams have been proposed and applied to the calculation of the ^{16}O binding energy in Ref. [89]. However, an investigation that fully exploits the advantages of an enlarged model space and analyzes the renormalizability of various power-counting scenarios for both nuclear matter and finite nuclei is so far absent.

We present here a first study where we apply such a strategy to both matter and finite nuclei, putting the basis for a novel approach to be adopted in nuclear structure

calculations. Our focus is indeed to develop a unified framework together with an order-by-order improvable and renormalizable interaction which has the potential to be applied to infinite nuclear matter and nuclei across the entire nuclear chart, as traditional EDF does.

LEADING ORDER: EMPIRICAL INTERACTIONS RENORMALIZED UNDER MEAN FIELD MODEL SPACE

We start by defining the Hamiltonian H_{LO} , which contains the kinetic term plus the LO interaction term V^{LO}

$$H_{LO} = \sum_i e_i \hat{n}_i + \sum_{i>j} V_{ij}^{LO}, \quad (1)$$

where e_i and \hat{n}_i are the energy and the particle-number operator for the particle i . The interaction term V_{ij}^{LO} is a two-body operator to be determined. To speculate a reasonable LO interaction under EDF, we make use of one basic requirement of EFT—the renormalizability of the observables. Studies performed for nuclear matter in Refs. [60, 61, 75] suggest that a $t_0 - t_3$ model of Skyrme-type interactions is most likely to be a suitable candidate for V^{LO} . MF calculations of Eq. (1) are straightforward for both nuclear matter and finite nuclei.

However, we do not adopt the conventional Hartree-Fock procedure here. Guided by empirical information (such as the information obtained by shell-model calculations fitted to experiments), one could start with an ansatz of the wavefunction Ψ and evaluate H_{LO} by calculating its matrix element. Note that here Ψ defines our model space at LO and does not change with the effective interaction. Ref. [90] showed that reasonably good results can be obtained by directly evaluating the Gogny interaction between Ψ consisting of a single-particle basis constructed in the shell model. Inspired by that, we directly define our LO model space as the shell-model wavefunction up to the highest occupied shell and calculate the expectation value of the Hamiltonian perturbatively. The ground-state (g.s.) energy of the system at LO can be written as $E_{g.s.}^{LO} = E_v + E_{coul} - t_{CM} + E_c$, with E_v, E_{coul}, E_c the energy of valence particles, the Coulomb, and the core contributions, respectively; $t_{CM} = \frac{3}{4}\hbar\omega$ is the center-of-mass (CM) kinetic energy. Throughout this exploratory work we only consider closed-shell nuclei, so that $E_v = 0$, and Coulomb is treated within mean-field approximation. The core energy can be further written as the core kinetic plus the core potential energy, that is $E_c = t_c + V_c$, where [90]

$$V_c = \sum_{j_a^c \leq j_b^c} \sum_{JT} (2T+1)(2J+1) \langle j_a^c j_b^c JT | V^{LO} | j_a^c j_b^c JT \rangle. \\ t_c = \sum_{j_a^c} (2T+1)(2J+1) \langle j_a^c | \hat{t} | j_a^c \rangle, \quad (2)$$

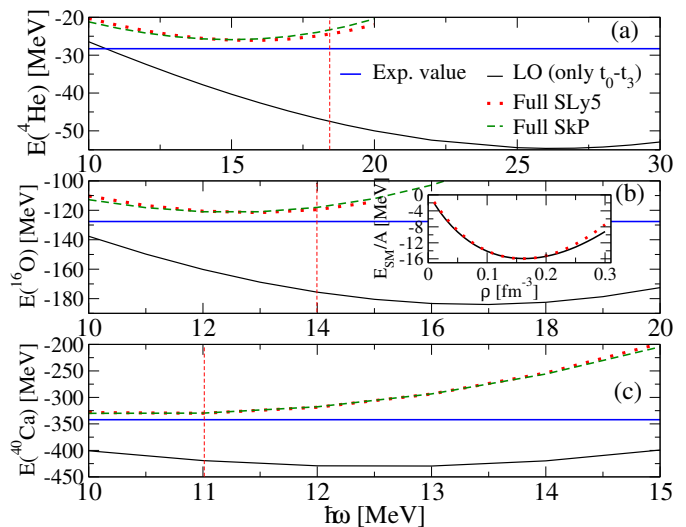


Figure 1. Ground state energies of ${}^4\text{He}$ (a), ${}^{16}\text{O}$ (b), and ${}^{40}\text{Ca}$ (c) as a function of $\hbar\omega$. Results obtained from a $t_0 - t_3$ model and full SLy5, and SkP functionals are plotted as black solid, red dotted, and green dashed lines, respectively. The empirical $\hbar\omega$ value for each nucleus is marked as a red vertical dashed line. The horizontal blue lines represent the experimental energies. The SM energy per particle at LO is plotted as a function of the density ρ in the inset.

Here j_a^c, j_b^c label the single-particle orbits in the core, \hat{t} is the kinetic energy operator; J and T are the total angular momentum and isospin quantum number for each pair of interacting particles, respectively.

Note that the combination of the harmonic oscillator (HO) strength $\hbar\omega$ and N_{max} (denoting the truncation up to the highest occupied shell) provides a natural cutoff of the Fermi sphere in finite nuclei and might play a similar role as the Fermi momentum k_F in the nuclear matter case. Since our interaction is singular, without additional regulators, results in general will not converge with the increase of $\hbar\omega$. For each nucleus, there exists an optimal $\hbar\omega$ so that the shell-model basis matches the size of the nucleus. For nuclei with mass number A , the empirical $\hbar\omega \approx 45A^{-1/3} - 25A^{-2/3}$ is frequently adopted [91]. With the above equations, evaluations of the g.s. the energy of ${}^4\text{He}$, ${}^{16}\text{O}$ and ${}^{40}\text{Ca}$ using V^{LO} are straightforward. The detailed derivation is given in Refs. [89, 90] and summarized in the supplemental materials, together with the form assumed by the adopted LO interaction.

We present the g.s. energies as a function of $\hbar\omega$ in Fig.1, where a $t_0 - t_3$ model of the SkP parametrization [92] is adopted for V^{LO} . LO calculations systematically provide strongly overbound nuclei with respect to experimental data, even at the empirical value of $\hbar\omega$, though the corresponding MF equation of state (EoS) for symmetric matter (SM) (shown in the inset of Fig.1) is quite satisfactory. This is not surprising judging from the simple form of the LO interaction. We have tried

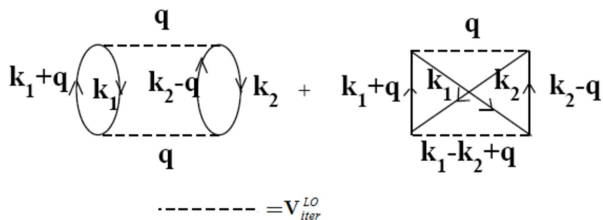


Figure 2. Once-iterated diagrams for the interaction V_{iter}^{LO} . \mathbf{k}_1 (\mathbf{k}_2) denotes the single-particle momentum of the initial (final) state, and \mathbf{q} is the transferred momentum.

other $t_0 - t_3$ parametrizations, which reproduce as well the empirical SM EoS, and found that the systematic overbinding persists. On the other hand, with the $t_{1,2}$ Skyrme terms included, the MF g.s. energies obtained from SkP [92] or SLy5 [93, 94] are very reasonable, with the minimum also located close to the empirical $\hbar\omega$ value. Although an EFT should aim to capture the most important physics already at LO, one could argue that basic physics is roughly captured once the equation of state of symmetric matter can be reproduced up to saturation density.

NEXT-TO-LEADING ORDER: TWO POSSIBILITIES OF IMPROVEMENTS

To improve further, two approaches are possible. First, one could add more terms to the effective interaction together with an EFT-based speculation on their form or importance, and then evaluate again Eq. (1) to produce better fits to a wider range of nuclear properties. Many attempts have been devoted toward this direction [69–73, 95–97]. On the other hand, since nuclei are bound-states, they should be generated by at least partial iteration of a certain interaction. The MF description might be then improved by considering higher-order corrections coming from the iterated diagrams, such as the ones corresponding to the enlargement of the model space through particle-hole excitations. Improvements in this direction are much less studied, as iterating effective interactions built at MF-level in the loops usually generates self-consistency problems, unless renormalization is taken care properly.

Starting from next-to-leading order (NLO), we im-

prove our theory by considering both of the above directions, and demonstrate how to establish self-consistent NLO corrections through proper renormalization procedures. Up to NLO, one has

$$E_{NLO} = E^{LO} + \langle \Psi | V_{ij}^{CT} | \Psi \rangle + E_{iter}^{NLO}, \quad (3)$$

where V_{ij}^{CT} is the higher-order contact interaction entering at NLO with its contribution evaluated at the MF level (the same way as in Eq. (2)). The structure of V_{ij}^{CT} has to be determined according to the renormalizability and the power-counting scheme. E_{iter}^{NLO} represents the contribution of the once-iterated diagrams listed in Fig. 2. The general form of E_{iter}^{NLO} reads [98]:

$$E_{iter}^{NLO} = -\frac{1}{4} \sum_{j_a^c \leq j_b^c, X_\alpha \leq X_\beta} \frac{|\langle j_a^c j_b^c JT | V_{iter}^{LO} | X_\alpha X_\beta JT \rangle|^2}{\varepsilon_\alpha + \varepsilon_\beta - \varepsilon_a - \varepsilon_b}, \quad (4)$$

where $j_{a(b)}^c$ are the same as in Eq. (2) because one stops at the highest occupied orbital; $X_{\alpha(\beta)}$ stands for excited states, where the summation starts at the Fermi sphere and stops at an upper limit which defines the second-order model space; $\varepsilon_i = k_i^2/2m$ is the single-particle energy of each state having momentum k_i (the effective mass is set to its bare value $m = 939$ MeV in this work). V_{iter}^{LO} denotes the part of the LO interaction which is iterated to provide the NLO contribution. A straightforward evaluation of Eq. (4) is in principle possible. However, the truncation applied to the excited states in the single-particle basis cannot be directly matched with the truncation performed for the EoS of matter in Refs. [60, 61, 75]—where a relative momentum cutoff Λ is applied. Moreover, Moshinsky transformations require all excited states $X_{\alpha,\beta}$ to be represented in terms of the HO basis¹, which complicates the matching between different nuclei, as they correspond to different $\hbar\omega$ and $X_{\alpha(\beta)}$.

To produce a renormalized interaction to be easily applied to all cases, we proceed as follows. First, since excitations are governed by V_{iter}^{LO} , one can directly represent the relevant wavefunctions in relative coordinates. Let us call $\mathbf{k}_1, \mathbf{k}_2$ ($\mathbf{k}'_1, \mathbf{k}'_2$) the single-particle momenta of the initial/final (intermediate) state. Then, the incoming and outgoing momenta in relative coordinates are $\mathbf{k} = (\mathbf{k}_1 - \mathbf{k}_2)/2$, $\mathbf{k}' = (\mathbf{k}'_1 - \mathbf{k}'_2)/2 + \mathbf{q}$, where \mathbf{q} is the transferred momentum. Eq. (4) can be rewritten as

$$E_{iter}^{NLO} = \frac{f(\hbar\omega)}{4} \left[\int d^3\mathbf{k} \int d^3\mathbf{k}' \int d^3\mathbf{K} \langle \Psi(\mathbf{K}; \mathbf{k}) | V_{iter}^{LO}(\mathbf{k}; \mathbf{k}') | \psi(\mathbf{k}') \rangle G \langle \psi(\mathbf{k}') | V_{iter}^{LO}(\mathbf{k}'; \mathbf{k}) | \Psi(\mathbf{K}; \mathbf{k}) \rangle \right]_{BC}. \quad (5)$$

¹ Alternatively, one could go through extra processes which involve

the decomposition of the chosen basis into the HO one [99, 100].

where

$$G = \frac{-m}{k'^2 - k^2}. \quad (6)$$

Ψ is represented in the same basis used at LO, which depends on the CM momentum $\mathbf{K} = \mathbf{k}_1 + \mathbf{k}_2 = \mathbf{k}'_1 + \mathbf{k}'_2$ and on the relative momentum \mathbf{k} . $\psi = \sum_i \phi_i$ denotes the intermediate excitations, where ϕ_i can be represented by any complete basis. One caveat is that if one chooses to expand Ψ and ψ in a different basis, an overall factor $f \neq 1$ will be needed to fix the norm. To define the intermediate model space, one must truncate it either by the number of basis states or by the highest momentum. In this work, we choose the second option and adopt the free wave-packets basis so that f depends only on $\hbar\omega$. The detailed derivation leading to Eq. (5) is given in the supplemental materials. Note that the conversion of initial/final and intermediate single-particle-basis states (which are also restricted as mentioned before) to relative coordinates results in a boundary condition (BC) which couples k_F to new variables \mathbf{k} , \mathbf{k}' and \mathbf{K} . The 3-folded integral under the same BC has been carried out to obtain the second-order EoS [62, 98], and is to be carried out in a similar manner in Eq. (5). However, unlike the nuclear matter case—where a clear definition of Fermi momentum is possible— k_F is not clearly given in finite nuclei. In the nuclear matter case, the radial integral dk is truncated by $k \in [0, k_F]$. On the other side, in finite nuclei, the same integrals are carried out through $k \in [0, \infty]$. However, the shell structure (the LO wavefunctions of a nucleus at a chosen $\hbar\omega$) provides a natural truncation analogous to k_F . To proceed, we interpret k_F in finite nuclei to be the highest momentum each wavefunction can access. The procedure to extract k_F in a finite nucleus is thus the following. First, we evaluate the g.s. energy at the MF level and separate the contributions from the t_0 , the t_3 , and the V^{CT} terms for each nucleus. Then, we compare the ratios $\frac{\langle t_0 \rangle}{\langle t_3 \rangle}$ and $\frac{\langle t_0 \rangle}{\langle V^{CT} \rangle}$ to their corresponding values in SM. The ratios in nuclear matter depend on k_F , whereas the same ratios in finite nuclei are related to their shell structure. By requiring the same ratios between finite nuclei and nuclear matter, we can extract the corresponding k_F for ${}^4\text{He}$, ${}^{16}\text{O}$ and ${}^{40}\text{Ca}$ (denoted as k_A) under various $\hbar\omega$ values. The resulting k_A are listed in Table I. One can see that a

$\hbar\omega$ (MeV)	11	12	13	14	15	16	17	18
k_A of ${}^4\text{He}$	0.90	0.95	0.98	1.02	1.05	1.08	1.12	1.15
k_A of ${}^{16}\text{O}$	1.08	1.13	1.18	1.22	1.26	1.30	1.34	1.38
k_A of ${}^{40}\text{Ca}$	1.25	1.37	1.35	1.40	1.45	1.49	1.54	1.58

Table I. k_A (unit: fm^{-1}) for ${}^4\text{He}$, ${}^{16}\text{O}$ and ${}^{40}\text{Ca}$ under various $\hbar\omega$. Those adopted in Fig. 3 are highlighted by bold text.

heavier nucleus (and a larger $\hbar\omega$) naturally corresponds

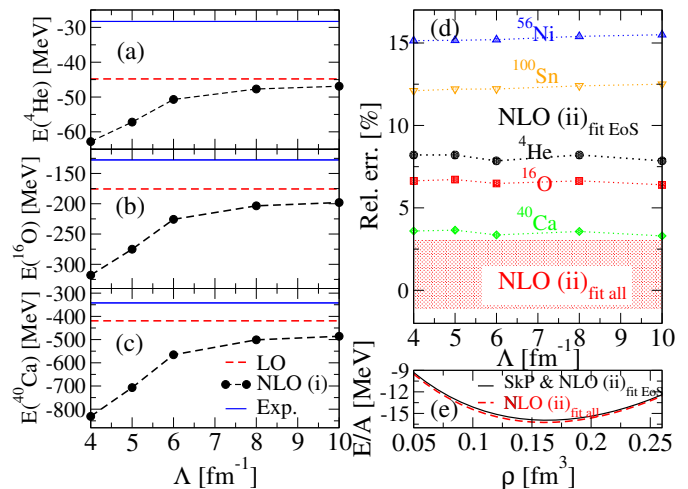


Figure 3. Left panels (a)-(c): Ground state energies up to NLO for ${}^4\text{He}$, ${}^{16}\text{O}$ and ${}^{40}\text{Ca}$ as a function of Λ . Right panel (d): Rel. err. = $(E_b - E_{exp.})/|E_{exp.}|$ for first five closed-shell, $N=Z$ nuclei. The labels NLO (i) and NLO (ii) refer to the two prescriptions described in the main text, where parameters in NLO (ii) are obtained by either fitted to EoS only (fit EoS) or an overall fit including EoS and all five nuclei (fit all). Their corresponding EoS are plotted in (e).

to a higher k_A . We have tried several interactions having different values of α (the power of the density in the t_3 term) and found a very weak spreading ($\leq 1\%$ variations for $\alpha \approx 0.16 - 0.3$)² between the values of k_A obtained by using such interactions in the matching of the ratios.

Once k_A is known, we have all the ingredients to perform actual calculations. In Refs. [61, 75], the full $t_0 - t_3$ LO interaction is iterated to generate E_{iter}^{NLO} for nuclear matter. The same procedure can be performed in principle in Eq. (5) for finite nuclei. However, some conceptual subtleties arise regarding how to account for the density ρ when one considers the fluctuation of the wavefunctions due to the intermediate excitations. In fact, in conventional EDF approaches with a density-dependent term included (for example the t_3 term of Skyrme interactions), the interaction does not correspond to a genuine Hamiltonian. The iteration of this term generates a conceptual drawback and may lead to technical problems such as divergences in BMF calculations for nuclei [101–103]. Also, the density-dependent term depends on the wavefunction and this could potentially complicate an EFT analysis. Therefore, we choose not to iterate the t_3 part of the interaction in this work.

In the following, we perform two types of NLO calculations:

- (i) Only the t_0 part of the LO interaction is iterated,

² For α up to 1, the extracted k_F can vary up to 5%.

and $V^{CT} = C(1 + x_c P_\sigma)$.

- (ii) Same as (i), but with additional $V_{ii}^{CT} = \frac{1}{2}t_1(1 + x_1 P_\sigma)(\mathbf{k}'^2 + \mathbf{k}^2) + t_2(1 + x_2 P_\sigma)\mathbf{k}' \cdot \mathbf{k}$, that is, the Skyrme-type $t_{1,2}$ terms are added.

Note that the above interactions are Skyrme-like, and $P_\sigma = (1 + \sigma_1 \sigma_2)/2$ is the spin-exchange operator. We treat C , x_c , α , $t_{0,1,2,3}$, and $x_{0,1,2,3}$ as the low-energy constants (LECs) in EFT, and we choose to renormalize them to reproduce the SLy5 SM and neutron matter (NM) EoSs. The LECs, the χ^2 values and the resulting EoSs are given in the supplemental materials. Predictions on g.s. energies of ${}^4\text{He}$, ${}^{16}\text{O}$, ${}^{40}\text{Ca}$, ${}^{56}\text{Ni}$ and ${}^{100}\text{Sn}$ evaluated up to NLO with $\Lambda = 4 - 10 \text{ fm}^{-1}$, are given in Fig.3, where the empirical $\hbar\omega = 45A^{-1/3} - 25A^{-2/3}$ are adopted. As one can see, the pathological overbinding trend at LO seems to persist under the prescription (i). Thus, without the entrance of new k_F -dependencies in the EoS (other than terms behave asymptotically $\sim k_F^4$ and proportional to t_0^2) at NLO, one does not observe any improvement from LO to NLO for both the EoS of matter and finite nuclei. Nevertheless, the NLO renormalizability is satisfied—which is reflected in the converging pattern of NLO (i) results against Λ . A real improvement is achieved by the prescription (ii), where, by just fitting to the empirical EoSs, reasonable reproductions of the experimental binding $E_{exp.}$ are found for nuclei up to mass number $A = 40$ (with $|\text{relative error}| = \frac{|E_b - E_{exp.}|}{|E_{exp.}|} \leq 8\%$, where E_b is the resulting binding energy). This suggests that the t_1 , t_2 terms are indeed indispensable, as indicated by many phenomenological studies. However, the error grows to $\sim 15\%$ when extending the calculation to the next two $N = Z$ nuclei (${}^{56}\text{Ni}$ and ${}^{100}\text{Sn}$). Note that the curves labelled as NLO (ii)_{fit EoS} are obtained by keeping the original SkP or SLy5 values of $t_{1,2,3}$, $x_{1,2,3}$ and α , while adjusting only t_0 , C and $x_{0,c}$ to two EoSs³. Up to NLO, the computational cost stays very closed to the MF calculations and is relatively small. Thus, we attempt a second fit (utilizing all LECs but keeping $\alpha = 1/6$) to the empirical EoSs and all five nuclei. We found it is possible to reproduce the experimental binding for all five nuclei within 3% (denoted by the red shaded area and labelled as NLO (ii)_{fit all} in Fig.3), if one allows the SM EoS to be slightly ($\leq 2\%$) more attractive around saturation than the one produced by SkP (panel (e), Fig.3).

POWER COUNTING: A PARTICLE-NUMBER-DEPENDENT HIGH- AND LOW-MOMENTUM SCALES

Finally, we speculate the high- and low-momentum scale M_{hi} and M_{lo} in our EFT-expansion. Since M_{lo} spans from 0 to k_F —which varies with A in a nucleus, a successful EFT arrangement of observables up to NLO in terms of powers series in (M_{lo}/M_{hi}) suggests that M_{hi} has the following properties:

- It is at least larger than k_F , and depends on the number of particles A .
- It depends on N_{max} and $\hbar\omega$, at least for those nuclei where central densities are lower than the saturation density of SM. Let us denote by A_s typical A values for which nuclei reach the saturation density in their central region. Then M_{hi} increases with A for $A < A_s$.

The breakdown scale has a functional form $M_{hi}(A, \hbar\omega)$. For $A < A_s$, the asymptotic form of the EFT expansion is $\frac{M_{lo}}{M_{hi}} \sim \frac{k}{\beta k_F(A)}$, where k is the characteristic center-of-mass momentum scale and $\beta \gtrsim 1$. On the other hand, $\beta k_F(A) \sim \bar{M}_{hi}$, that is, becomes a constant for $A > A_s$, where \bar{M}_{hi} is a hard breakdown scale to be extracted by a Lepage-like plot [104, 105] from NLO and next-to-next-to-leading order (NNLO) results; $\frac{2}{3\pi^2}\bar{M}_{hi}^3$ and $\frac{1}{3\pi^2}\bar{M}_{hi}^3$ correspond to the highest density ρ for which one can trust the EoS of SM and NM, respectively (for example, twice the saturation density of SM).

SUMMARY

In summary, we provide a novel framework to include BMF correlations order by order. With a reliable extraction of k_F , the treatment of finite nuclei and nuclear matter can be performed on the same footing. Investigations up to NLO are performed for five $N = Z$ closed-shell nuclei and for nuclear matter for the first time. We have tested various arrangements of NLO corrections through renormalization-group analysis. Note that our analysis are based on a trial and error procedure. Since not all possibilities are tested, our NLO prescription (ii) might still be subjected to further refinements. Nevertheless, the trial and error procedure carried out in present work—which checks the renormalizability of the in-medium loops (and therefore the self-consistency of the proposed beyond mean field corrections)—can be repeated with different interactions in the future. Thus, our work serves as a starting point toward an EFT-based description of nuclei across the entire nuclear chart. Many interesting future works including the treatment of higher-order correlations and a full EFT power-counting analysis are in progress.

³ LECs adjusted to SkP and SLy5 EoSs produce $\leq 1\%$ difference in E_b up to ${}^{40}\text{Ca}$, and are indistinguishable in Fig.3.

This work was supported by the Czech Science Foundation GACR grant 19-19640S and 22-14497S, the Swedish Research Council (Grant number 2017-04234), the European Research Council (ERC) under the European Union's Horizon 2020 research and innovation programme (Grant agreement number 758027). Computational resources were supplied by the project "e-Infrastruktura CZ" (e-INFRA CZ LM2018140) supported by the Ministry of Education, Youth and Sports of the Czech Republic, IT4Innovations at Czech National Supercomputing Center under project number OPEN-24-21 1892, and the Swedish National Infrastructure for Computing (SNIC) at Chalmers Centre for Computational Science and Engineering (C3SE), and the National Supercomputer Centre (NSC) partially funded by the Swedish Research Council. S. B. acknowledges support from the Alexander von Humboldt foundation.

-
- [1] S. Weinberg, *Physics Letters B* **251**, 288 (1990).
 [2] S. Weinberg, *Nuclear Physics B* **363**, 3 (1991).
 [3] C. Ordóñez, L. Ray, and U. van Kolck, *Physical Review Letters* **72**, 1982 (1994).
 [4] C. Ordóñez, L. Ray, and U. van Kolck, *Physical Review C* **53**, 2086 (1996).
 [5] E. Epelbaum, W. Glöckle, and U.-G. Meissner, *Nuclear Physics A* **637**, 107–134 (1998).
 [6] E. Epelbaum, W. Glöckle, and U.-G. Meissner, *Nuclear Physics A* **671**, 295–331 (2000).
 [7] D. Entem and R. Machleidt, *Physics Letters B* **524**, 93–98 (2002).
 [8] D. R. Entem and R. Machleidt, *Physical Review C* **66** (2002), 10.1103/physrevc.66.014002.
 [9] E. Epelbaum, W. Glöckle, and U.-G. Meissner, *Nuclear Physics A* **747**, 362–424 (2005).
 [10] E. Epelbaum, H. Krebs, and U. G. Meißner, *Eur. Phys. J. A* **51**, 53 (2015), arXiv:1412.0142 [nucl-th].
 [11] U. V. Kolck, *Progress in Particle and Nuclear Physics* **43**, 337–418 (1999).
 [12] P. F. Bedaque and U. V. Kolck, *Annual Review of Nuclear and Particle Science* **52**, 339–396 (2002).
 [13] E. Epelbaum, H.-W. Hammer, and U.-G. Meissner, *Reviews of Modern Physics* **81**, 1773–1825 (2009).
 [14] H.-W. Hammer, S. König, and U. van Kolck, *Reviews of Modern Physics* **92** (2020), 10.1103/revmodphys.92.025004.
 [15] W. H. Dickhoff and C. Barbieri, *Prog. Part. Nucl. Phys.* **52**, 377 (2004).
 [16] D. Lee, *Progress in Particle and Nuclear Physics* **63**, 117 (2009).
 [17] S. K. Bogner, R. J. Furnstahl, and A. Schwenk, *Prog. Part. Nucl. Phys.* **65**, 94 (2010).
 [18] B. R. Barrett, P. Navrátil, and J. P. Vary, *Prog. Part. Nucl. Phys.* **69**, 131 (2013).
 [19] A. Carbone, A. Cipollone, C. Barbieri, A. Rios, and A. Polls, *Phys. Rev. C* **88**, 054326 (2013), arXiv:1310.3688 [nucl-th].
 [20] G. Hagen, T. Papenbrock, M. Hjorth-Jensen, and D. J. Dean, *Rep. Prog. Phys.* **77**, 096302 (2014).
 [21] H. Hergert, S. Bogner, T. Morris, A. Schwenk, and K. Tsukiyama, *Physics Reports* **621**, 165 (2016), memorial Volume in Honor of Gerald E. Brown.
 [22] J. Carlson, S. Gandolfi, F. Pederiva, S. C. Pieper, R. Schiavilla, K. E. Schmidt, and R. B. Wiringa, *Rev. Mod. Phys.* **87**, 1067 (2015).
 [23] N. Barnea, W. Leidemann, and G. Orlandini, *Nuclear Physics A* **650**, 427 (1999).
 [24] W. Glöckle, H. Witala, D. Hüber, H. Kamada, and J. Golak, *Physics Reports* **274**, 107 (1996).
 [25] I. Stetcu, B. R. Barrett, P. Navrátil, and J. P. Vary, *Phys. Rev. C* **71**, 044325 (2005).
 [26] I. Stetcu, B. R. Barrett, and U. van Kolck, *Physics Letters B* **653**, 358 (2007).
 [27] I. Stetcu, B. R. Barrett, U. van Kolck, and J. P. Vary, *Phys. Rev. A* **76**, 063613 (2007).
 [28] I. Stetcu, J. Rotureau, B. R. Barrett, and U. van Kolck, *Journal of Physics G: Nuclear and Particle Physics* **37**, 064033 (2010).
 [29] J. Rotureau, I. Stetcu, B. R. Barrett, M. C. Birse, and U. van Kolck, *Phys. Rev. A* **82**, 032711 (2010).
 [30] I. Stetcu, J. Rotureau, B. R. Barrett, and U. van Kolck, *Annals of Physics* **325**, 1644 (2010).
 [31] J. Rotureau, I. Stetcu, B. R. Barrett, and U. van Kolck, *Phys. Rev. C* **85**, 034003 (2012).
 [32] S. Binder, A. Ekström, G. Hagen, T. Papenbrock, and K. A. Wendt, *Phys. Rev. C* **93**, 044332 (2016).
 [33] X. Zhang, S. Stroberg, P. Navrátil, C. Gwak, J. Melendez, R. Furnstahl, and J. Holt, *Phys. Rev. Lett.* **125**, 112503 (2020), arXiv:2004.13575 [nucl-th].
 [34] C.-J. Yang, *Physical Review C* **94** (2016), 10.1103/physrevc.94.064004.
 [35] R. Roth, A. Calci, J. Langhammer, and S. Binder, *Phys. Rev. C* **90**, 024325 (2014).
 [36] S. K. Bogner, T. T. S. Kuo, and A. Schwenk, *Physics Reports* **386**, 1 (2003).
 [37] S. K. Bogner, R. J. Furnstahl, and R. J. Perry, *Phys. Rev. C* **75**, 061001 (2007).
 [38] U. van Kolck, *Front. in Phys.* **8** (2020), 10.3389/fphy.2020.00079.
 [39] E. Epelbaum and J. Gegelia, *Eur. Phys. J. A* **41**, 341 (2009).
 [40] H. W. Griesshammer, *Few Body Syst.* **63**, 44 (2022), arXiv:2111.00930 [nucl-th].
 [41] U. van Kolck, *Few Body Syst.* **62**, 85 (2021), arXiv:2107.11675 [nucl-th].
 [42] C. J. Yang, A. Ekström, C. Forssén, and G. Hagen, *Phys. Rev. C* **103**, 054304 (2021), arXiv:2011.11584 [nucl-th].
 [43] C. J. Yang, *European Physical Journal A* **56**, 96 (2020).
 [44] C. J. Yang, A. Ekström, C. Forssén, G. Hagen, G. Rupak, and U. van Kolck, (2021), arXiv:2109.13303 [nucl-th].
 [45] D. Gambacurta, M. Grasso, and J. Engel, *Phys. Rev. C* **92**, 034303 (2015).
 [46] D. Gambacurta, M. Grasso, and J. Engel, *Phys. Rev. Lett.* **125**, 212501 (2020).
 [47] C. Robin and E. Litvinova, *Phys. Rev. C* **98**, 051301 (2018).
 [48] C. Robin and E. Litvinova, *Phys. Rev. Lett.* **123**, 202501 (2019).
 [49] Y. F. Niu, G. Colò, and E. Vigezzi, *Phys. Rev. C* **90**, 054328 (2014).

- [50] G. Colò, P. F. Bortignon, M. Brenna, X. Roca-Maza, E. Vigezzi, K. Moghrabi, M. Grasso, and K. Mizuyama, *Phys. Scripta* **89**, 054006 (2014).
- [51] G. Colò, H. Sagawa, and P. F. Bortignon, *Phys. Rev. C* **82**, 064307 (2010).
- [52] S. Burrello, J. Bonnard, and M. Grasso, *Phys. Rev. C* **103**, 064317 (2021).
- [53] S. Burrello, M. Colonna, G. Colò, D. Lacroix, X. Roca-Maza, G. Scamps, and H. Zheng, *Phys. Rev. C* **99**, 054314 (2019).
- [54] S. Burrello, M. Colonna, and H. Zheng, *Frontiers in Physics* **7**, 53 (2019).
- [55] H. Hammer and R. Furnstahl, *Nucl. Phys. A* **678**, 277 (2000), arXiv:nucl-th/0004043.
- [56] N. Kaiser, *J. Phys. G* **42**, 095111 (2015), arXiv:1505.07095 [nucl-th].
- [57] N. Kaiser, *Eur. Phys. J. A* **53**, 104 (2017), arXiv:1703.07745 [nucl-th].
- [58] K. Moghrabi, M. Grasso, G. Colo, and N. Van Giai, *Phys. Rev. Lett.* **105**, 262501 (2010), arXiv:1012.3097 [nucl-th].
- [59] K. Moghrabi, (2016), arXiv:1607.05829 [nucl-th].
- [60] C. J. Yang, M. Grasso, K. Moghrabi, and U. van Kolck, *Phys. Rev. C* **95**, 054325 (2017), arXiv:1312.5949 [nucl-th].
- [61] C. Yang, M. Grasso, and D. Lacroix, *Phys. Rev. C* **94**, 031301 (2016), arXiv:1604.06587 [nucl-th].
- [62] C. Yang, M. Grasso, X. Roca-Maza, G. Colò, and K. Moghrabi, *Phys. Rev. C* **94**, 034311 (2016), arXiv:1604.06278 [nucl-th].
- [63] D. Lacroix, A. Boulet, M. Grasso, and C.-J. Yang, *Phys. Rev. C* **95**, 054306 (2017), arXiv:1704.08454 [nucl-th].
- [64] M. Grasso, D. Lacroix, and C. Yang, *Phys. Rev. C* **95**, 054327 (2017), arXiv:1704.08510 [nucl-th].
- [65] C. J. Yang, M. Grasso, and D. Lacroix, *Phys. Rev. C* **96**, 034318 (2017), arXiv:1706.00258 [nucl-th].
- [66] J. Bonnard, M. Grasso, and D. Lacroix, *Phys. Rev. C* **101**, 064319 (2020), arXiv:2001.08082 [nucl-th].
- [67] M. Grasso, *Prog. Part. Nucl. Phys.* **106**, 256 (2019), arXiv:1811.01039 [nucl-th].
- [68] J. Bonnard, M. Grasso, and D. Lacroix, *Phys. Rev. C* **98**, 034319 (2018), arXiv:1806.01084 [nucl-th].
- [69] H. Gil, P. Papakonstantinou, C. H. Hyun, T.-S. Park, and Y. Oh, *Acta Phys. Polon. B* **48**, 305 (2017), arXiv:1611.04257 [nucl-th].
- [70] H. Gil, Y. Oh, C. H. Hyun, and P. Papakonstantinou, *New Phys. Sae Mulli* **67**, 456 (2017).
- [71] H. Gil, P. Papakonstantinou, C. H. Hyun, and Y. Oh, *JPS Conf. Proc.* **20**, 011041 (2018).
- [72] H. Gil, Y.-M. Kim, C. H. Hyun, P. Papakonstantinou, and Y. Oh, *Phys. Rev. C* **100**, 014312 (2019), arXiv:1903.04123 [nucl-th].
- [73] H. Gil, Y.-M. Kim, P. Papakonstantinou, and C. Ho, *Phys. Rev. C* **103**, 034330 (2021), arXiv:2010.13354 [nucl-th].
- [74] R. J. Furnstahl, *Eur. Phys. J. A* **56**, 85 (2020), arXiv:1906.00833 [nucl-th].
- [75] S. Burrello, M. Grasso, and C.-J. Yang, *Physics Letters B* **811**, 135938 (2020).
- [76] F. Marino, C. Barbieri, A. Carbone, G. Colò, A. Lovato, F. Pederiva, X. Roca-Maza, and E. Vigezzi, *Phys. Rev. C* **104**, 024315 (2021).
- [77] G. De Gregorio, F. Knapp, N. L. Iudice, and P. Veselý, *Phys. Rev. C* **105**, 024326 (2022), arXiv:2202.10266 [nucl-th].
- [78] F. Androozzi, F. Knapp, N. L. Iudice, A. Porrino, and J. Kvasil, *Phys. Rev. C* **75**, 044312 (2007).
- [79] F. Androozzi, F. Knapp, N. L. Iudice, A. Porrino, and J. Kvasil, *Phys. Rev. C* **78**, 054308 (2008).
- [80] D. Bianco, F. Knapp, N. Lo Iudice, F. Androozzi, and A. Porrino, *Phys. Rev. C* **85**, 014313 (2012).
- [81] G. De Gregorio, F. Knapp, N. Lo Iudice, and P. Veselý, *Phys. Rev. C* **93**, 044314 (2016).
- [82] G. De Gregorio, F. Knapp, N. Lo Iudice, and P. Veselý, *Phys. Rev. C* **94**, 061301 (2016).
- [83] G. De Gregorio, F. Knapp, N. Lo Iudice, and P. Veselý, *Phys. Rev. C* **95**, 034327 (2017).
- [84] G. D. Gregorio, F. Knapp, N. L. Iudice, and P. Veselý, *Physica Scripta* **92**, 074003 (2017).
- [85] G. De Gregorio, F. Knapp, N. Lo Iudice, and P. Veselý, *Phys. Rev. C* **97**, 034311 (2018).
- [86] G. De Gregorio, F. Knapp, N. Lo Iudice, and P. Veselý, *Phys. Rev. C* **99**, 014316 (2019).
- [87] G. De Gregorio, F. Knapp, N. Lo Iudice, and P. Veselý, *Phys. Rev. C* **101**, 024308 (2020).
- [88] G. De Gregorio, F. Knapp, N. Lo Iudice, and P. Veselý, *Phys. Lett. B* **821**, 136636 (2021).
- [89] M. Brenna, G. Colò, and X. Roca-Maza, *Physical Review C* **90** (2014), 10.1103/physrevc.90.044316.
- [90] W. G. Jiang, B. S. Hu, Z. H. Sun, and F. R. Xu, *Physical Review C* **98** (2018), 10.1103/physrevc.98.044320.
- [91] J. Blomqvist and A. Molinari, *Nucl. Phys. A* **106**, 545 (1968).
- [92] J. Dobaczewski, H. Flocard, and J. Treiner, *Nuclear Physics A* **422**, 103 (1984).
- [93] E. Chabanat, P. Bonche, P. Haensel, J. Meyer, and R. Schaeffer, *Nuclear Physics A* **627**, 710 (1997).
- [94] E. Chabanat, P. Bonche, P. Haensel, J. Meyer, and R. Schaeffer, *Nucl. Phys. A* **635**, 231 (1998), [Erratum: *Nucl. Phys. A* 643, 441–441 (1998)].
- [95] P. Becker, D. Davesne, J. Meyer, J. Navarro, and A. Pastore, *Phys. Rev. C* **96**, 044330 (2017).
- [96] K. Bennaceur, A. Idini, J. Dobaczewski, P. Dobaczewski, M. Kortelainen, and F. Raimondi, *Journal of Physics G: Nuclear and Particle Physics* **44**, 045106 (2017).
- [97] D. Davesne, J. Navarro, J. Meyer, K. Bennaceur, and A. Pastore, *Phys. Rev. C* **97**, 044304 (2018).
- [98] K. Davies and M. Baranger, *Nucl. Phys. A* **120**, 254 (1968).
- [99] G. Papadimitriou, B. R. Barrett, J. Rotureau, N. Michel, and M. Płoszajczak, *EPJ Web of Conferences* **66**, 02006 (2014).
- [100] G. Papadimitriou, J. Rotureau, N. Michel, M. Płoszajczak, and B. R. Barrett, *Physical Review C* **88** (2013), 10.1103/physrevc.88.044318.
- [101] D. Lacroix, T. Duguet, and M. Bender, *Phys. Rev. C* **79**, 044318 (2009).
- [102] M. Bender, T. Duguet, and D. Lacroix, *Phys. Rev. C* **79**, 044319 (2009).
- [103] T. Duguet, M. Bender, K. Bennaceur, D. Lacroix, and T. Lesinski, *Phys. Rev. C* **79**, 044320 (2009).
- [104] H. W. Griebhammer, In 8th International Workshop on Chiral Dynamics (CD) Pisa, Italy, June 29-July 3, CD2015 PoS(CD15)104, arXiv:1511.00490v3 [nucl-th] (2015).

- [105] H. W. Griesshammer, [European Physical Journal A](#) **56** (2020), [10.1140/epja/s10050-020-00129-5](#).
- [106] R. Lawson, Theory of the nuclear shell model (Clarendon Press, Oxford, 1980).

SUPPLEMENTAL MATERIAL

**TWO-BODY MATRIX ELEMENTS AT
MEAN-FIELD LEVEL**

In the shell model, the j - j coupling scheme is commonly adopted. However, the two-body Skyrme- or Gogny-type effective interactions operate in the L - S coupling (partial-wave) scheme. Therefore, the following transformation is needed[106],

$$|(n_a l_a j_a)(n_b l_b j_b) J J_z\rangle = \sum_{\lambda S} \sum_{\mu S_z} \gamma_{\lambda S}^{(J)}(j_a l_a; j_b l_b) \langle \lambda \mu S S_z | J J_z \rangle \times |(n_a l_a m_a)(n_b l_b m_b) \lambda \mu \rangle | S S_z \rangle, \quad (7)$$

where $\langle \lambda \mu S S_z | J J_z \rangle$ are the standard Clebsch-Gordan coefficients and

$$\gamma_{\lambda S}^{(J)}(j_a l_a; j_b l_b) = \sqrt{(2j_a + 1)(2j_b + 1)(2S + 1)(2\lambda + 1)} \times \begin{Bmatrix} l_a & 1/2 & j_a \\ l_b & 1/2 & j_b \\ \lambda & S & J \end{Bmatrix}. \quad (8)$$

Here J and J_z denote the total angular momentum and its z -component, respectively, and S and S_z are the total intrinsic spin and its z -component, respectively.

One could rewrite the two-particle wavefunctions in the laboratory coordinates with quantum numbers $(J J_z T)$ in terms of wavefunctions in relative coordinates, that is,

$$|(n_a l_a j_a)(n_b l_b j_b) J J_z T\rangle = \sum_{nlNL} \sum_{mM} \sum_{\mu S_z} \sum_{\lambda S} \gamma_{\lambda S}^{(J)}(j_a l_a; j_b l_b) \frac{1 - (-1)^{S+T+l}}{\sqrt{2(1 + \delta_{n_a n_b} \delta_{l_a l_b} \delta_{j_a j_b})}} \times M_{\lambda}(nlNL; n_a l_a n_b l_b) \langle l m L M | \lambda \mu \rangle \langle \lambda \mu S S_z | J J_z \rangle \times |nlm\rangle |NLM\rangle |SS_z\rangle |T\rangle, \quad (9)$$

where $|T\rangle$ is the two-particle isospin eigenstate with a total isospin T . Finally, the full expression of the two-body

matrix element of an effective interaction V_{NN} reads

$$\begin{aligned} & \langle (n_a l_a j_a)(n_b l_b j_b) J J_z T | V_{NN} | (n_c l_c j_c)(n_d l_d j_d) J J_z T \rangle \\ &= \sum_{n'l'N'L'} \sum_{nlNL} \sum_{m'M'} \sum_{mM} \sum_{\mu'S'_z} \sum_{\mu S_z} \sum_{\lambda'S'} \sum_{\lambda S} \tilde{\gamma}_{\lambda'S'}^{(J)}(j_a l_a; j_b l_b) \\ & \times \tilde{\gamma}_{\lambda S}^{(J)}(j_c l_c; j_d l_d) M_{\lambda'}(n'l'N'L'; n_a l_a n_b l_b) \\ & \times M_{\lambda}(nlNL; n_c l_c n_d l_d) \langle l' m' L' M' | \lambda' \mu' \rangle \\ & \times \langle \lambda' \mu' S' S'_z | J J_z \rangle \langle l m L M | \lambda \mu \rangle \langle \lambda \mu S S_z | J J_z \rangle \\ & \times \langle T | \langle S' S'_z | \langle N' L' M' | \langle n' l' m' | V_{NN} | n l m \rangle | N L M \rangle \\ & \times | S S_z \rangle | T \rangle, \end{aligned} \quad (10)$$

with $\tilde{\gamma}_{\lambda S}^{(J)}(j_a l_a; j_b l_b) = \frac{1 - (-1)^{S+T+l}}{\sqrt{2(1 + \delta_{n_a n_b} \delta_{l_a l_b} \delta_{j_a j_b})}} \gamma_{\lambda S}^{(J)}(j_a l_a; j_b l_b)$, where symbols with prime refer to the left vector. Note that if V_{NN} consists only of s -waves, then the kernel $\langle n' l' m' | V_{NN} | n l m \rangle$ can be further simplified into:

$$\begin{aligned} & \langle n' 0 m' | V_{NN,12} | n 0 m \rangle \\ &= \frac{1}{2\pi^2} \int_0^\infty p^2 dp \int_0^\infty p'^2 dp' \psi_{n' 0 m'}(p) V_{0,0s=j}(p, p') \psi_{n 0 m}(p'). \end{aligned} \quad (11)$$

Here $V_{0,0s=j}(p, p')$ is the s -wave component of V_{NN} , and $\psi_{nl=0m}$ is the standard Harmonic oscillator (HO) wavefunction with quantum numbers n, l, m . In the above expression, we have assumed that V_{NN} is density independent. For density-dependent effective interactions (such as the Skyrme one), one may follow Eqs. (4)-(7) in Ref.[90] to perform the integral over the CM coordinate space $\mathbf{R} = (\mathbf{r}_1 + \mathbf{r}_2)/2$ and to evaluate the matrix element of $\langle N' L' M' | \hat{\rho}(\mathbf{R}) | N L M \rangle$. Here $\hat{\rho}(\mathbf{R})$ is proportional to the modular square of the CM part of the wavefunction, with details given in Ref.[90].

The LO interaction adopted in this work has the following form:

$$V_{12}^{LO} = \delta(\mathbf{r}_1 - \mathbf{r}_2) t_0 (1 + x_0 P_\sigma) + \delta(\mathbf{r}_1 - \mathbf{r}_2) \frac{t_3}{6} (1 + x_3 P_\sigma) \rho^\alpha, \quad (12)$$

where t_0, t_3, x_0, x_3 , and α are parameters, $\rho = \rho(\frac{\mathbf{r}_1 + \mathbf{r}_2}{2})$ is the density, and $P_\sigma = (1 + \sigma_1 \sigma_2)/2$ is the spin-exchange operator.

Note that Eq. (10) can be reduced to a simpler form in the case of infinity nuclear matter, where the system becomes homogeneous so that it can be described by a Fermi gas with wavefunction Ψ consisting of free wavepackets u_k labelled by the momentum k . Within a box volume Ω , Eq. (10) becomes

$$\sum_{u_k, u_p} \sum_{JT} (2T + 1)(2J + 1) \langle u_k | V_{NN} | u_p \rangle, \quad (13)$$

where the sum up to the highest occupied orbitals can be converted into integrals up to the Fermi momentum k_F , that is

$$\sum_{u_k, u_p} \langle u_k | V_{NN} | u_p \rangle = \frac{\Omega^2}{(2\pi)^6} \int_0^{k_F} k^2 dk \int d\theta_k \int d\phi_k \int_0^{k_F} p^2 dp \int d\theta_p \int d\phi_p \frac{V_{NN}(\mathbf{k}, \mathbf{p})}{\Omega}. \quad (14)$$

ONCE-ITERATED MATRIX ELEMENTS

The matrix elements of the interaction given in the main text have exactly the same form as Eq. (10) here, by replacing the inner kernel $\langle N' L' M' | \langle n' l' m' | V_{NN} | n l m \rangle | N L M \rangle$ with

$$\frac{1}{4} \sum_{N'' L'' M'' n'' l'' m''} \langle N' L' M' | \langle n' l' m' | V_{iter}^{LO} | n'' l'' m'' \rangle | N'' L'' M'' \rangle \times G \langle N'' L'' M'' | \langle n'' l'' m'' | V_{iter}^{LO} | n l m \rangle | N L M \rangle, \quad (15)$$

where G is given by Eq. (6) in the main text. For a density-independent interaction, the non-vanishing matrix elements in Eq. (15) have quantum numbers $N' = N$, $L' = L$ and $M' = M$. Furthermore, for the s -wave part of the effective interaction $V_{iter}^{LO} = t_0(1 + x_0 P_\sigma)$ considered in this work, we have $n' = n$ and $l' = l = m' = m = 0$ due to the energy conservation property of the Moshinsky transformations. In addition, one can further drop the summation regarding the CM intermediate states $\langle N'' L'' M'' |$ as their overlap is always 1. Thus, the inner kernel (excluding the external $\langle N L M |$ and $| N L M \rangle$)

$$-\frac{m}{4} \frac{(4\pi)^3}{(2\pi)^9} \left[\int_0^{2k_F} K^2 dK \int_0^{k_F} k^2 dk \int_0^\Lambda k'^2 dk' \frac{\Psi_{NLM}^{HO}(K) \psi_{n00}^{HO}(k) [t_0(1 + x_0 P_\sigma)]^2 \psi_{n00}^{HO}(k) \Psi_{NLM}^{HO}(K)}{k'^2 - k^2} \right]_{BC}. \quad (18)$$

The dK integral is not equal to 1 and the denominator does not diverge, due to the fact that the three variables $\mathbf{k} = (\mathbf{k}_1 - \mathbf{k}_2)/2$, $\mathbf{k}' = (\mathbf{k}'_1 - \mathbf{k}'_2)/2 = (\mathbf{k}_1 - \mathbf{k}_2)/2 + \mathbf{q}$, and $\mathbf{K} = \mathbf{k}_1 + \mathbf{k}_2 = \mathbf{k}'_1 + \mathbf{k}'_2$ are restricted by the following BC:

$$\begin{aligned} |\mathbf{k}_1| < k_F, |\mathbf{k}_2| < k_F, \\ |\mathbf{q} + \mathbf{k}_1| > k_F, |\mathbf{k}_2 - \mathbf{q}| > k_F. \end{aligned} \quad (19)$$

A detailed illustration of the above BC and the related treatments to perform the triple integral can be found in Fig.2 and Fig.3 of Ref.[98].

We note that the results for finite nuclei obtained with the above equations correspond to the full expressions given in Eqs. (22) and (27) in Ref.[62] for the EoS. The expressions of second-order EoSs listed in Refs.[58, 60, 61, 75] are the asymptotic form after expanding the results in power series of Λ . Whereas an analytic result of the triple integral can be obtained for the EoS of matter, Eq. (18)

becomes:

$$\begin{aligned} & \frac{1}{4} \sum_{n''00} \langle n00 | V_{iter}^{LO} | n''00 \rangle G \langle n''00 | V_{iter}^{LO} | n00 \rangle \\ & = \frac{1}{4} \sum_{\alpha} \langle n00 | V_{iter}^{LO} | \alpha \rangle G \langle \alpha | V_{iter}^{LO} | n00 \rangle. \end{aligned} \quad (16)$$

Note that we have taken the freedom to re-express the intermediate states from the HO-basis in relative coordinates into any complete set $\sum_{\alpha} |\alpha\rangle \langle \alpha|$ within the same coordinates, where $|\alpha\rangle$ labels the eigenstates. One can then choose the new basis to be the kinetic eigenstates so that $|\alpha\rangle = |u_k\rangle$ and the summation \sum_{α} is converted into an integral over the intermediate momentum k' . At the same time, one can also decompose each outer HO-wavefunction $\langle n00 | k \rangle$ into a linear combination of $\sum_k c_k u_k$, with $c_k = \psi_{n00}^{HO}(k)$. In this way, Eq. (16) becomes

$$-\frac{m}{4} \frac{(4\pi)^2}{(2\pi)^6} \int_0^{k_F} k^2 dk \int_0^\Lambda k'^2 dk' \frac{\psi_{n00}^{HO}(k) [t_0(1 + x_0 P_\sigma)]^2 \psi_{n00}^{HO}(k)}{k'^2 - k^2}. \quad (17)$$

Note that, together with the outer integral on $\langle N L M |$, Eq. (15) becomes

can only be solved numerically for finite nuclei. Although the asymptotic form agrees with the full expression at $\Lambda \rightarrow \infty$, the discrepancies between them can be up to 10% for lower cutoff values ($\Lambda \leq 6 \text{ fm}^{-1}$). Therefore, we always adopt the full expression in the nuclear matter calculations carried out throughout this work.

TABLES OF RENORMALIZED LOW-ENERGY CONSTANTS

We list below the LECs up to NLO based on the prescriptions (i)-(ii) as described in the main text. Note that here C^Λ and $C^{\Lambda*}$ are related to $V^{CT} = C(1 + x_c P_\sigma)$ by

$$\begin{aligned} C &= C^\Lambda \\ x_c &= 1 - \frac{C^{\Lambda*}}{C^\Lambda}. \end{aligned} \quad (20)$$

Λ (fm $^{-1}$)	4	5	6	8	10
t_0 (fm 2)	1.349	-1.732	-2.189	-1.546	-1.307
t_3 (fm $^{2+3\alpha}$)	96.393	40.434	53.091	59.182	60.729
x_0	-2.468	-1.459	-0.188	-0.480	-0.738
x_3	4.188	2.050	0.567	0.479	0.474
α	0.0358	0.218	0.274	0.291	0.289
C^Λ (fm 2)	-10.994	2.578	-0.631	-2.616	-2.241
C^{Λ^*} (fm 2)	53.597	21.767	5.281	5.208	7.456
χ^2	15.1	30.2	289	334	356

Table II. χ^2 and adjusted parameters based on the prescription (i) obtained for $\Lambda =$ values from 2 to 10 fm $^{-1}$.

Λ (fm $^{-1}$)	4	5	6	8	10
t_0 (fm 2)	-0.173	-0.169	-0.141	-0.0868	-0.139
t_1 (fm 4)	2.448	2.448	2.448	2.448	2.448
t_2 (fm 4)	-2.784	-2.784	-2.784	-2.784	-2.784
t_3 (fm $^{2+3\alpha}$)	69.747	69.747	69.747	69.747	69.747
x_0	-0.243	-0.115	-0.312	1.387	-0.051
x_1	-0.328	-0.328	-0.328	-0.328	-0.328
x_2	-1.0	-1.0	-1.0	-1.0	-1.0
x_3	1.267	1.267	1.267	1.267	1.267
α	0.167	0.167	0.167	0.167	0.167
C^Λ (fm 2)	-12.40	-12.398	-12.427	-12.468	-12.410
C^{Λ^*} (fm 2)	-2.556	-2.579	-2.573	-2.827	-2.605
χ^2	$7.6 \cdot 10^{-3}$	$3.5 \cdot 10^{-3}$	$2.5 \cdot 10^{-3}$	$8.1 \cdot 10^{-4}$	$6.4 \cdot 10^{-4}$

Table III. χ^2 and parameters based on prescription (ii) obtained from $\Lambda = 2$ to 10 fm $^{-1}$. Note that at nuclear matter level we have adopted the empirical EoSs to be those given by the SLy5-mean-field.

The corresponding EoSs generated by LECs listed in Tables II-IV are plotted as Figs.4-6.

Finally, we list the LECs correspond to NLO (ii) $_{\text{fit all}}$ in Table IV.

Λ (fm $^{-1}$)	4	5	6	8	10
t_0 (fm 2)	-0.183	-0.154	-0.123	-0.069	0.130
t_1 (fm 4)	1.625	1.625	1.625	1.625	1.625
t_2 (fm 4)	-1.710	-1.710	-1.710	-1.710	-1.710
t_3 (fm $^{2+3\alpha}$)	94.811	94.811	94.811	94.811	94.811
x_0	-0.230	-0.099	-0.159	-0.309	1.699
x_1	0.653	0.653	0.653	0.653	0.653
x_2	-0.537	-0.537	-0.537	-0.537	-0.537
x_3	0.181	0.181	0.181	0.181	0.181
α	0.167	0.167	0.167	0.167	0.167
C^Λ (fm 2)	-14.653	-14.678	-14.717	-14.781	-14.849
C^{Λ^*} (fm 2)	-10.263	-10.327	-10.350	-10.410	-10.405
χ^2	$9.7 \cdot 10^{-3}$	$3.5 \cdot 10^{-2}$	$2.4 \cdot 10^{-3}$	$6.1 \cdot 10^{-3}$	$2.2 \cdot 10^{-2}$

Table IV. χ^2 and parameters based on prescription (ii) obtained from $\Lambda = 2$ to 10 fm $^{-1}$. Note that at nuclear matter level we have adopted the empirical EoSs to be those given by the SkP-mean-field.

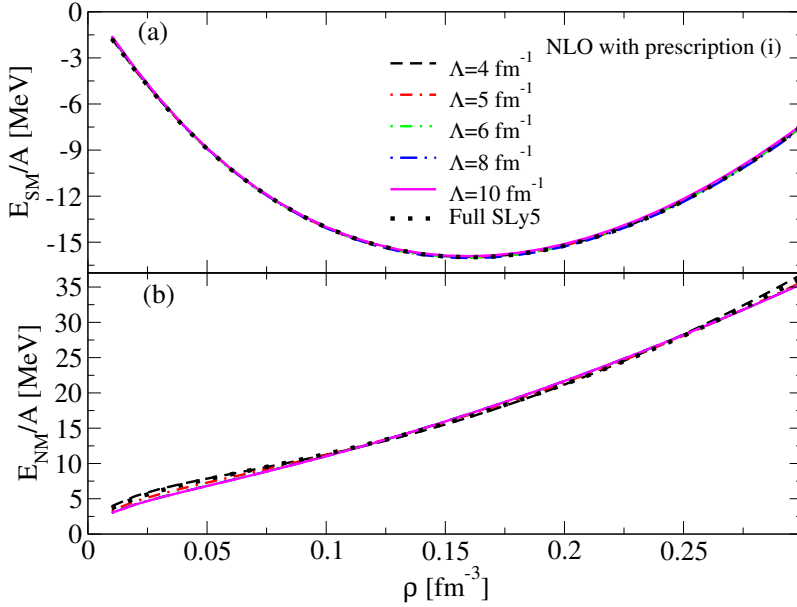


Figure 4. Second-order EOSs for SM (a) and NM (b) under the prescription (i) adjusted on the full SLy5-mean-field EOSs, with an effective mass equal to the bare mass, for different values of the cutoff.

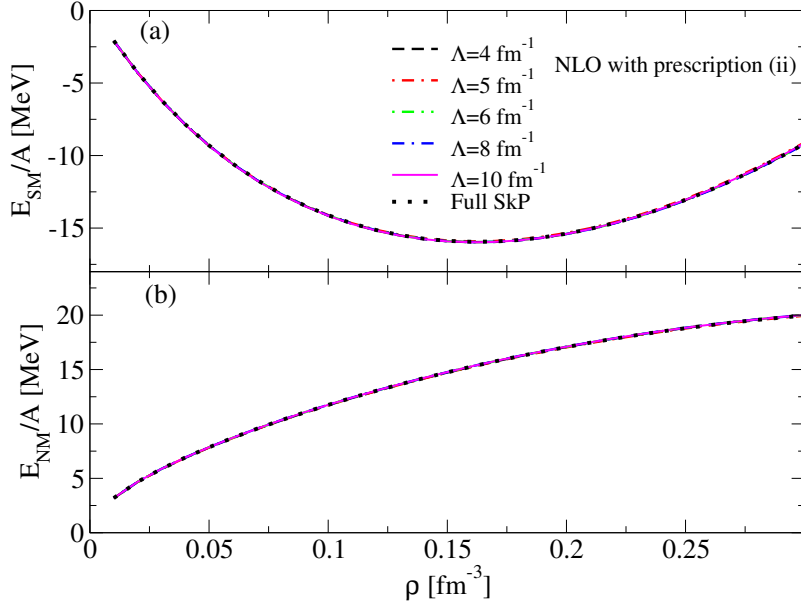


Figure 5. Second-order EOSs for SM (a) and pure NM (b) under the prescription (ii) adjusted on the full SkP-mean-field EOSs, with an effective mass equal to the bare mass, for different values of the cutoff.

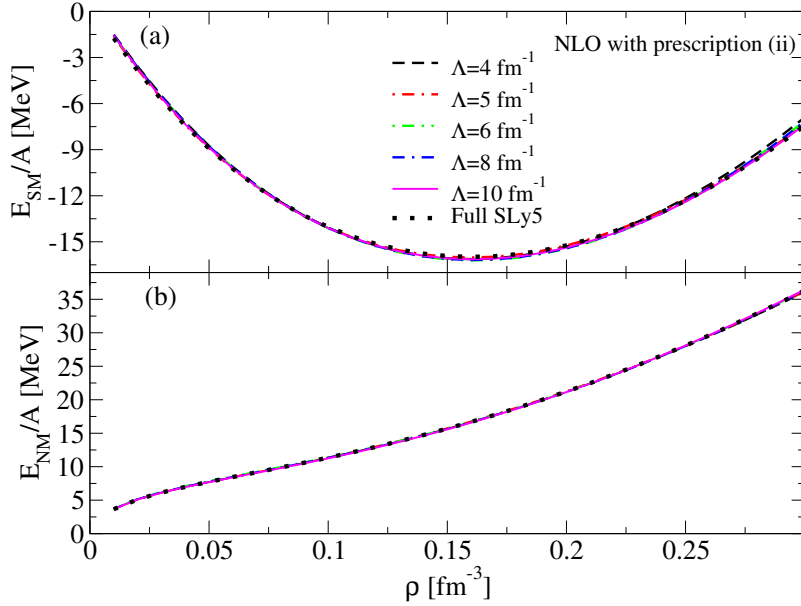


Figure 6. Second-order EOSs for SM (a) and pure NM (b) under prescription (ii) adjusted on the full SLy5-mean-field EOSs, with an effective mass equal to the bare mass, for different values of the cutoff.

Λ (fm ⁻¹)	4	6	8	10
t_0 (fm ²)	-4.96	-4.36	-3.72	-3.62
t_1 (fm ⁴)	-1.06	-0.076	0.15	0.16
t_2 (fm ⁴)	-7.49	-8.79	-9.06	-8.61
t_3 (fm ^{2+3α)}	35.81	48.09	45.09	61.96
x_0	-0.20	-0.13	-0.62	-0.47
x_1	-3.15	-61.93	49.55	40.72
x_2	-0.91	-1.02	-1.04	-1.04
x_3	2.33	1.29	1.66	0.95
α	0.167	0.167	0.167	0.167
C^Λ (fm ²)	16.8	19.1	27.7	28.1
$C^{\Lambda*}$ (fm ²)	35.2	33.9	69.2	65.1

Table V. Parameters of NLO (ii)_{fit all} obtained from $\Lambda = 4$ to 10 fm^{-1} . Note that for all Λ , they produce symmetric EoSs which are consistently more attractive ($\sim 2\%$) than the SkP-mean-field value around saturation density, as shown in Fig.3 (e) in the main text.